Hindawi
Journal of Nanomaterials
Volume 2020, Article ID 2057097, 11 pages
https://doi.org/10.1155/2020/2057097

Research Article

Characterization and Application of Carboxymethyl Chitosan-Based Bioink in Cartilage Tissue Engineering

Yunfan He,[1] **Soroosh Derakhshanfar**,[1,2] **Wen Zhong**,[3] **Bingyun Li**,[4] **Feng Lu**,[1] **Malcolm Xing**,[1,2] **and Xiaojian Li**[1]

[1]*Department of Plastic and Cosmetic Surgery, Nanfang Hospital, Southern Medical University, Guangzhou, Guangdong, China*
[2]*Department of Mechanical Engineering, University of Manitoba, Winnipeg, Canada*
[3]*Department of Biosystems Engineering, University of Manitoba, Winnipeg, Canada*
[4]*Department of Orthopaedics, School of Medicine, West Virginia University, Morgantown, WV, USA*

Correspondence should be addressed to Feng Lu; doctorlufeng@hotmail.com, Malcolm Xing; malcolm.xing@umanitoba.ca, and Xiaojian Li; lixj1999@smu.edu.cn

Received 10 June 2019; Revised 5 November 2019; Accepted 11 December 2019; Published 12 March 2020

Academic Editor: Silvia Licoccia

Chitosan is a promising natural biomaterial for biological application; however, the weak mechanical performance of pristine chitosan limits its further utilization in hard tissue (such as cartilage) engineering. In this study, a chitosan-based 3D printing bioink with suitable mechanical properties was developed as 3D bioprinting ink for chondrocyte support. Chitosan was first modified by ethylenediaminetetraacetic acid (EDTA) to provide more carboxyl groups followed by physical crosslinking with calcium to increase the hydrogel strength. Dynamic mechanical analysis was carried out to evaluate viscoelastic properties with the addition of modified chitosan. A bioink with a combination of modified and pristine chitosan was formulated for scaffold fabrication via 3D bioprinting technique. Furthermore, cell viability, cell proliferation, and expression of chondrogenic markers were evaluated *in vitro* in chondrocytes loaded on the bioink. The novel bioink exhibited a favorable mechanical property and promoted cell attachment and chondrogenic gene expression in chondrocytes. Based on these results, we can conclude that the presented bioink could qualify for use in 3D bioprinting in cartilage tissue engineering.

1. Introduction

Tissue engineering is currently an attractive and fast-developing research field focusing on restoration and regeneration of damaged tissues and organs. Researchers often consider cells, scaffolds, and growth factors as the main components in tissue engineering. A controlled 3D structure loaded with cells allows for specific distribution of cells and therefore results in improved cell proliferation and tissue regeneration. To this end, 3D printing, also known as additive manufacturing, has been used to construct 3D structures mimicking the nature of tissue [1, 2], and it is now one of the most attractive research topics in biomedical and tissue engineering fields [3, 4]. The importance of bioprinting arises from providing biomedical end users the ability to print scaffolds in required size and configurations with manipulated physical and chemical properties. Despite that numerous promising formulas have been revealed to date, printable inks with board source, facile manufacture process, and tunable mechanical properties for a variety of biomedical utilizations have continued to be a challenge [1, 5]. It has been demonstrated previously that cell behavior and tissue generation are affected by material properties such as stiffness and degradation [6–8]. Therefore, developing new tunable 3D printable inks can lead to significant advances in scaffold configuration for tissue engineering [9, 10]. Similar to bulk hydrogel synthesis, chemical crosslinking and physical crosslinking are also adapted to 3D bioprinting.

Although chemical crosslinking after extrusion has been widely employed, many of the chemical crosslinking agents are toxic and result in adverse reactions in the hydrogel [11]. For instance, glutaraldehyde, formaldehyde, and carbodiimide

are recognized for their cytotoxicity in gelatin-based hydrogels [12, 13]. By contrast, physical crosslinking constitutes a preferred alternative due to facile process and low cytotoxicity. Nevertheless, the intrinsic property of pristine materials should be considered for the enhancement of biomedical application; for instance, it has been shown that alginate-nanofibrillated cellulose (NFC) can be used as a cell-compatible bioink combining fast gelation properties of alginate and good shear thinning properties of NFC [14]. However, alginate hydrogels require complementary side groups to improve cell adhesion [15]. Chitosan, a nature-derived polysaccharide, has gained increased attention as a biomaterial during the past decade, which is attributable to its excellent biocompatibility and biodegradability [15]. Cartilage is an avascular tissue consisting of a small number of chondrocytes (10–15%) with limited self-regenerative properties [16, 17], and there is a critical need for tissue engineering to generate a scaffold to serve as a matrix for new cartilage formation. The characteristics of chitosan are similar to those of hyaluronic acid and glycosaminoglycans which are distributed extensively in native cartilage, and the degraded products of chitosan are involved in chondrification [18, 19]. However, the weak mechanical property of pristine chitosan limited its further utilization in cartilage regeneration, and the poor water solubility hinders the large-scale use. Therefore, the development of 3D printable chitosan ink with enhanced mechanical properties that could be used to print 3D hydrogel templates for chondrocyte culture and cartilage engineering was investigated in this study. Herein, carboxymethyl chitosan, which is water soluble at neutral pH values, was employed due to the physiological status of cells. Moreover, the stability and mechanical properties of chitosan hydrogels were enhanced by complementation with carboxyl groups, through the addition of ethylenediaminetetraacetic acid (EDTA), and physical crosslinking via calcium solution. The physical crosslinking administered in this work also eliminated concerns over cytotoxicity associated with chemical crosslinking. Mechanical performance and 3D printability of the bioink were investigated, and the *in vitro* proliferation and chondrogenesis of chondrocytes loaded on 3D printed chitosan hydrogel were determined.

2. Materials and Methods

2.1. Materials. Carboxymethyl chitosan, ultrapure grade EDTA free acid (292.25 g/mol), and 1-ethyl-3-(3-dimethylaminopropyl)carbodiimide hydrochloride (EDC-HCl, 191.7 g/mol) were purchased from Clearsynth, Amresco, and ProteoChem, respectively. The 3D bioprinter used in this study was from Hkable 3D.

2.2. Mechanical Characterization and Swelling Ratio Measurement. The Discovery HR-1 hybrid rheometer (TA Instruments) with a Peltier plate (20 mm) was used to evaluate the rheological properties of the bioink. Shear rate was swept from 0.1 to 100 s^{-1} for shear viscosity measurement, and frequency was swept from 0.1 to 200 rad·s^{-1} for storage and loss modulus evaluation. The Instron 5965 Dual Column Tabletop Testing System was used to evaluate the compressive strength of the hydrogel. All measurements were performed at 22°C. Fourier transform infrared spectroscopy (FTIR) characterization was conducted with the iS10 FTIR spectrophotometer (Thermo Fisher Scientific Inc., MA, USA). Samples of unmodified carboxymethyl chitosan, modified chitosan (CE), and hydrogel were lyophilized and analyzed at wavelength ranging from 4000 to 400 cm^{-1}. ^1H NMR experiment was carried out by the Bruker Avance 300 MHz NMR spectrometer with relaxation delay setting at 2 s to reveal the chemical structure. The related samples were lyophilized and dissolved in D_2O at 10 mg/ml.

Table 1: Composition of the studied formulations.

Chitosan : CE ratio	Chitosan (%*w*/*v*)	CE (%*w*/*v*)
C9CE1.6	9	1.6
C10.6CE1.6	10.6	1.6
C13.4CE1.6	13.4	1.6
C21CE1.6	21	1.6

Swelling ratio in bioink samples crosslinked with four concentrations of calcium solution ranging from 0.1 M to 2 M was measured. Hydrogels were weighed (W_1) before immersion in distilled water and weighed (W_2) multiple times over a period of 22 days. The mass swelling ratio were calculated using the following equation: $\text{swelling ratio} = (W_2 - W_1)/W_1 \times 100\%$.

2.3. Hydrogel Preparation. Carboxymethyl chitosan (200 mg) was dissolved in 10 ml of double-distilled water, and 240 mg of EDTA free acid was added to the solution. Furthermore, 160 mg of EDC-HCl was added as a carboxyl activating agent to form amine bonds in the solution, and the reaction mixture was incubated at 25°C under constant stirring overnight. The solution was later purified using dialysis tubing for 2 days, and the resulting solution was freeze-dried for 72 h. The final puffy powder produced, referred to as CE (chitosan-EDTA), was used as the primary precursor for printing ink. To prepare the printable hydrogel precursor, the CE solution was supplemented with additional chitosan to increase the ink viscosity and the ratio of chitosan added to the CE powder (chitosan : CE) in the final step before printing was slightly changed to tune the mechanical properties of the hydrogel (Table 1). The mixture was under constant stirring for 2 h to produce the final printable precursor which was centrifuged at 3000 rpm for 5 min to remove the bubbles. After printing, calcium chloride solutions with concentrations ranging from 0.1 M to 2 M were used as the crosslinking agent. A schematic presentation of the hydrogel preparation is depicted in Figures 1(a) and 1(b).

2.4. Printing Method. The method used for printing the bioink developed in the present work is a combination of pneumatic and piston-driven methods (Hkable 3D). The bioink goes through an extrusion process in order to print 3D constructs through layer-by-layer deposition of biomaterial. The thickness and the width of each layer can be tuned by tuning printing speed, extruder needle size, and air pressure applied to the piston. The printed structure may be

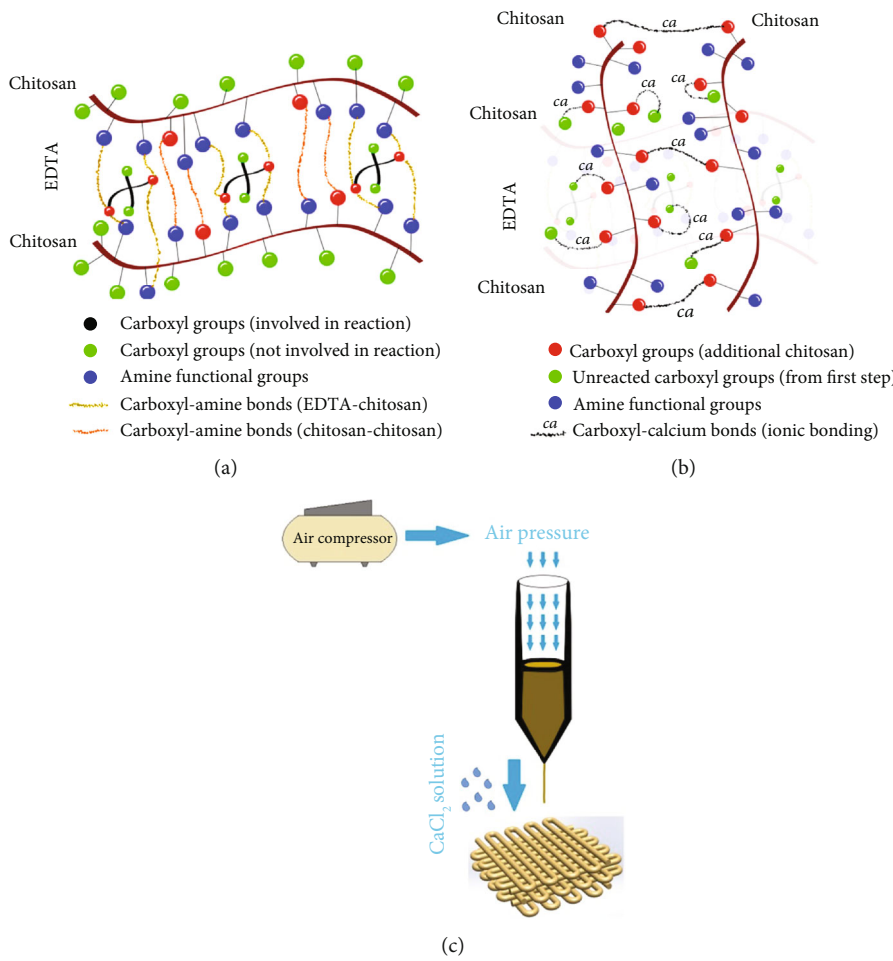

Figure 1: Schematic diagram of hydrogel preparation and printing. (a) First step: chitosan reacting with EDTA, unreacted carboxyl groups (green) take part in the next step. (b) Second step: additional chitosan is added to the solution and crosslinked with $CaCl_2$ solution after printing to form hydrogel. (c) Hydrogel printing method.

composed of as many layers as needed. In order to maintain the continuity of printed hydrogel line and prevent clogging at the extruder, the diameter of the needle used for 3D printing in this work was 0.5 mm, the air pressure was controlled by an affiliated precise regulator and set at 110 psi, and the travel speed of the extruder was set to 300 mm/min.

2.5. Isolation and Cell Seeding of Rabbit Chondrocytes. Rabbit chondrocytes were used to investigate the effects of the chitosan scaffold on cell viability, proliferation, and differentiation. To obtain primary chondrocytes, macroscopically intact rabbit cartilage was harvested, minced, and soaked for 1 h with 2 mg/ml protease, followed by overnight incubation with 1.5 mg/ml type II collagenase (Catalog number: 17101015, Thermo Fisher Scientific, USA) in a 37°C incubator. After centrifugation and filtration, primary chondrocytes were harvested.

For cell seeding, prepared chitosan hydrogel scaffolds were placed in a 12-well cell culture cluster. After that, 1 ml of complete media containing the cells (1×10^5) was directly pipetted onto each scaffold and cultured at 37°C in 5% CO_2 in a humidified atmosphere. Cells cultured in wells without hydrogel scaffolds served as the control.

2.6. Assessment of Cell Viability. Cell viability was assessed by the LIVE/DEAD Viability/Cytotoxicity Kit (Catalog number: L3224, Invitrogen, UK) and quantified by flow cytometry measurement. After 36 h incubation on chitosan scaffold, cells were collected and stained with dyed with propidium iodide/Annexin V-FITC Apoptosis Detection Kit (Thermo Fisher Scientific Inc., MA, USA) to evaluate the percentage of live cells.

2.7. Proliferation Assay. After seeding the cells on the scaffolds for 36 h, cellular proliferation was measured using the Cell-Light EdU Apollo 567 *in vitro* Imaging Kit (RiboBio, Guangzhou, China) according to the manufacturer's instructions. 4′,6-Diamidino-2-phenylindole (DAPI) was used to stain the cellular nuclei. Proliferation indicator 5-ethynyl-2′-deoxyuridine (EdU) incorporated into the nucleus of chondrocytes was detected by fluorescence microscopy (Nikon Corp.). The chondrocyte proliferation rate was assessed by counting the percentage of EdU-labeled cells in DAPI-labeled cells in five fields of each scaffold.

2.8. Reverse Transcription-Quantitative Polymerase Chain Reaction (RT-qPCR) Analysis. RNA was isolated from seeded

chondrocytes at different time points using TRIzol Reagent (Invitrogen Life Technologies, Carlsbad, California) according to the manufacturer's protocol, followed by reverse transcription. RT-qPCR was carried out according to the TaqMan method with previously designed primers (Thermo Fisher Scientific) and was used for gene expression analysis. Relative expressions were calculated by cycle threshold method using ACTB as an endogenous reference gene. The primers used to amplify messenger RNA sequences are listed in Table 2.

2.9. Statistical Analysis. Data are expressed as mean ± SEM and analyzed using IBM SPSS Version 21.0 software (IBM Corp., Armonk, NY). Repeated-measures analysis of variance was used to analyze the results. Furthermore, an independent t-test was used to compare two groups at a single time point. Meanwhile, one-way analysis of variance was used to compare groups at all the time points. A p value < 0.05 indicated statistical significance.

3. Results and Discussion

3.1. Characterization of Chitosan-Chemical Structures (FTIR and NMR Analysis). FTIR spectra of carboxymethyl chitosan in Figure 2(b) show strong absorption peaks around 3426 cm^{-1} which are attributed to the presence of OH stretching vibrations. The peak around 2924 cm^{-1} is due to the presence of C-H stretching vibrations; two peaks around 1657 and 1567 cm^{-1} can be attributed to N-H bending vibration and C=O groups of anionic carboxylates, respectively. The second spectrum of CE shows the appearance of a peak around 1723 cm^{-1} which is characteristic of C=O vibration of carboxylic acid and a strong peak at 1652 cm^{-1} which is attributed to the carbonyl stretching of amide vibrations. These bands suggest a successful coupling between EDTA and carboxymethyl of chitosan. The third spectrum shows the disappearance of a peak at 1710 cm^{-1} and the appearance of a band at 1633 cm^{-1}. These observations confirm the chelation of calcium to EDTA via O-H of the carboxylic acid functionality. The appearance of a band at 1633 cm^{-1} is in fact the shift of a peak at 1652 cm^{-1}, suggesting the presence of calcium in the form of metal complex with chitosan-EDTA. In addition, the three spectra showing the peak at 1410 cm^{-1} are assigned to the bending vibrations of the methylene protons of the CH_2COOH groups. The peaks in the range 1156 to 1068 cm^{-1} are attributed to C-O-C of the ring and the C-O stretching vibrations, respectively. The FTIR spectra confirm the successful coupling between carboxymethyl chitosan and EDTA as well as the formation of calcium complex with CE.

The ^{1}H NMR spectrum at 300 MHz was carried out in D_2O. The results (Figure 2(c)) show that the resonance proton at 7.90 ppm belongs to the amide proton. The proton H_1 appeared at 4.65 ppm, and the proton resonance H_3 to H_6 appeared at 3.6–3.9 ppm. The presence of the proton H_a at 2.3 ppm and the proton H_b at 3.40 ppm suggests the successful coupling of EDTA with the carboxymethyl chitosan. The ^{1}H NMR confirms the coupling between EDTA and CMC.

Table 2: The primers of collagen II and Sox 9.

Genes	Primers
Collagen II	Forward: AGCGGTGACTACTGGATAGA
	Reverse: CTGCTCCACCAGTTCTTCTT
Sox 9	Forward: CCACCTCTCTTACCTCTCTCAT
	Reverse: GGACAGCTTACAAGGGTTTCT

3.2. Specification of the Bioinks. In the present study, printable ink consists of two main components, CE and subsequently added chitosan. Additional chitosan provides more polymer chains to adjust the viscosity of the bioink for extrusion bioprinting. The carboxyl groups on different chains form insufficient ionic bonding with calcium as well as with certain carboxyl groups left unreacted from the CE powder. Therefore, the amounts of the two main components were modified to find the proper viscosity and concentration for a successful printing and gelation of the precursor. As the amount of these two components were varied, the bioink printability and gelation quality were affected. A few pictures of samples printed with different mixture ratios and the final printed sample with high printing precision are shown in Figure 3(a) to illustrate this step. It is important to note that because the focus of this work was to develop a bioink suitable for 3D bioprinting, the bioink ratio found to be accurately printable (90 : 10) was evaluated specifically in all plots.

Another essential factor to be considered is the ability to print multiple layers in order to construct complex structures. Figure 3(b) displays the optical microscope images of printed multilayered structures showing the ability of the present bioink to print complex structures consisting of multilayer straight and arced printed filaments.

Rheology, which is the study of flow of matter under external forces, is notably important in bioprinting and biofabrication [1]. Various rheological parameters, such as viscosity and shear thinning, influence the biofabrication process and therefore need to be investigated. To begin with, viscosity, the resistance of a hydrogel precursor under external forces, is determined primarily by the solution concentration and the molecular weight of the polymers. Higher concentrations generally mean higher viscosity and denser polymer networks that could potentially hinder favorable cell proliferation and tissue formation [20]. However, low concentrations negatively affect shape fidelity after deposition of hydrogel and the printed strands spread out on the printing substrate.

To investigate the change in properties due to altered composition, four bioinks were formulated and investigated with regard to rheological and mechanical properties. Four chitosan : CE ratios (namely, 93 : 07, 90 : 10, 87 : 13, and 85 : 15) were studied and compared.

In these samples, the weight of the CE powder in the solution was kept constant, whereas the weight of the additional chitosan was slightly changed. As depicted in Figure 4(a), higher proportions of CE in the solution resulted in higher storage and loss modulus. Similar to a previous study involving the use of nanofibrillated cellulose [14], CE was the main

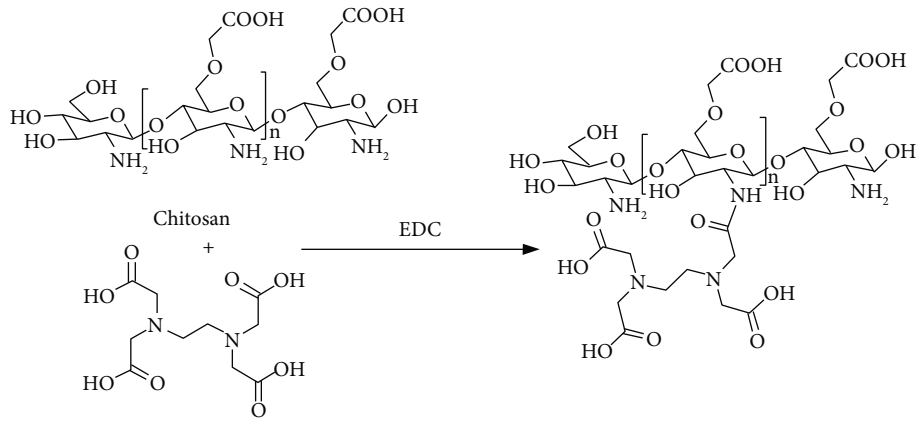

(a)

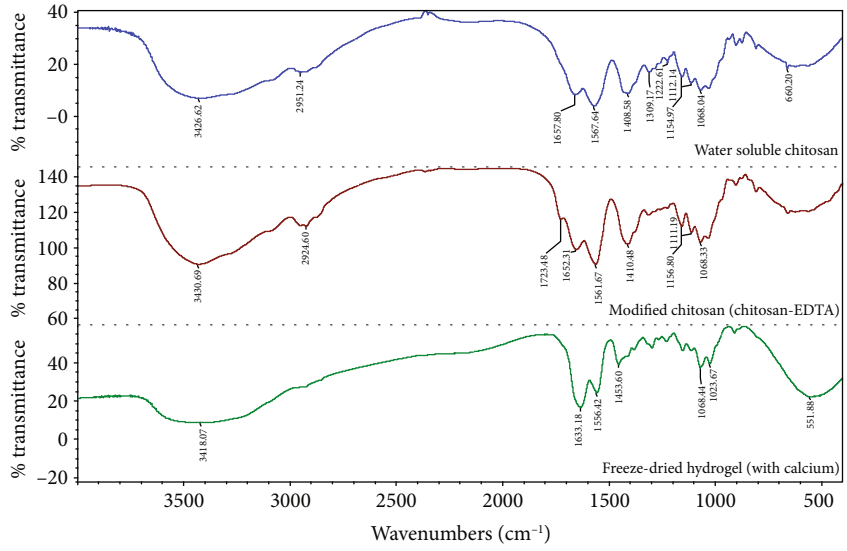

(b)

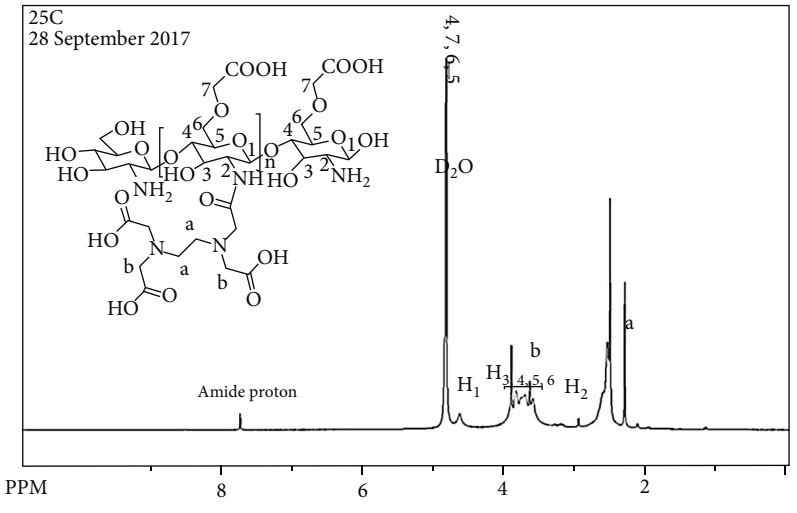

(c)

Figure 2: (a) Schematic diagram of chemical synthesis of modified chitosan. (b) FTIR spectra: top image: carboxymethyl chitosan without any modification, middle image: modified chitosan, and bottom image: freeze-dried hydrogel (after gelation by adding 1 M calcium solution). (c) ^{1}H NMR spectrum of the EDTA-modified chitosan hydrogel network at 300 MHz. The chitosan/CE conjugate ratio of the samples tested is 90 : 10.

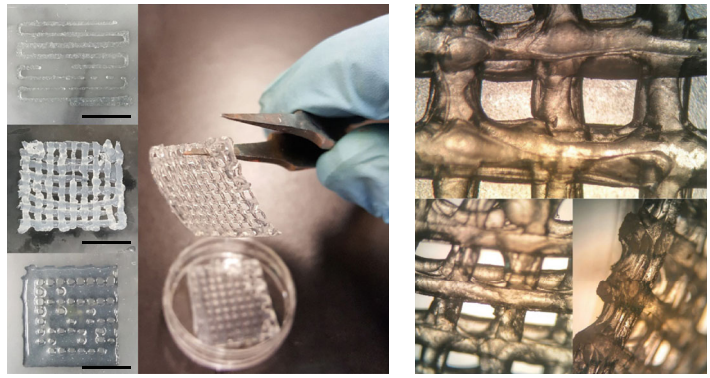

(a) (b)

Figure 3: (a) Printed samples with different chitosan : modified chitosan (CE) ratios. Images on the left, from top to bottom, show highly viscous bioink resulting in a discontinuous print, highly viscous bioink printed using a large diameter needle resulting in an inaccurate print, and low-viscous bioink incapable of holding its shape after printing. Image on the right shows an accurate printed structure with a chitosan : CE ratio of 90 : 10. (b) Micrographs of a printed five-layer hydrogel from various angles, showing the bonding of the layers. The chitosan/CE conjugate ratio of the sample shown is 90 : 10. The mesh size is 25 × 25 mm, and the diameter of the printing needle is 0.5 mm. Scale bar = 1 cm.

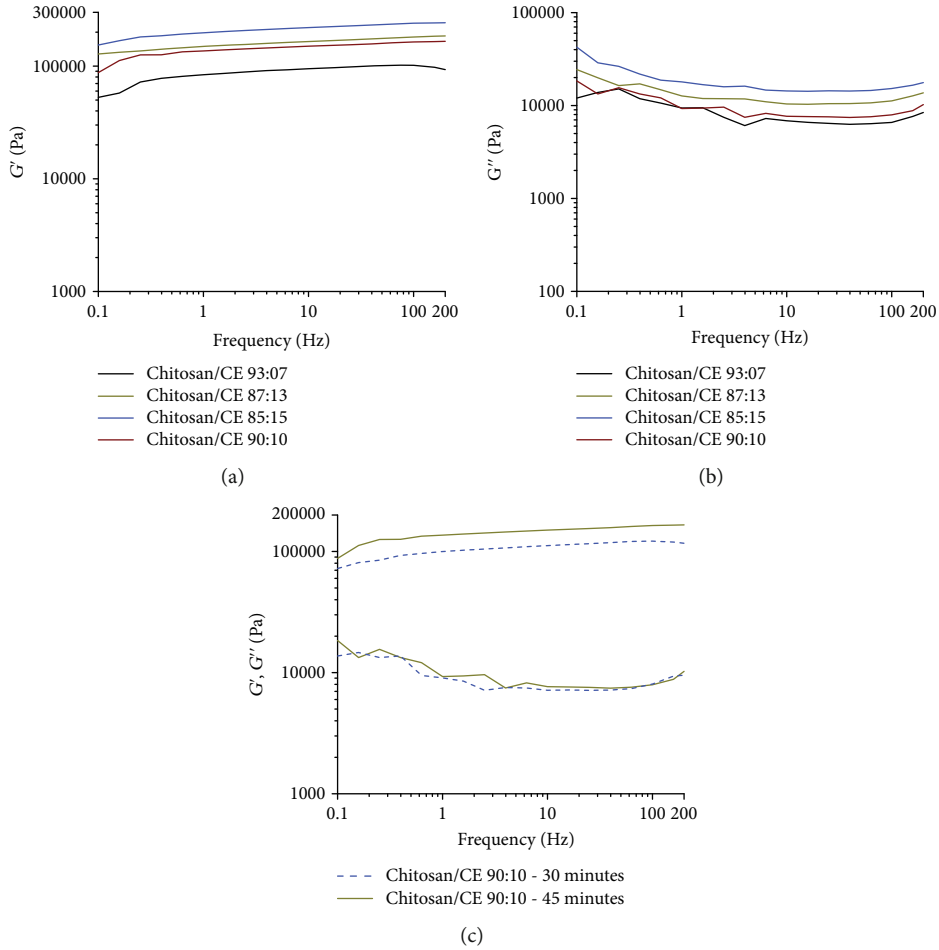

Figure 4: (a) Storage and (b) loss modulus of chitosan/CE hydrogel. Four Chitosan/CE conjugate ratios tested. (c) Storage modulus (G') and loss modulus (G'') of the bioink as a function of crosslinking time. Solid lines represent 45 min of crosslinking, and dashed lines represent 30 min of crosslinking. $CaCl_2$ (1 M) solution is used as the crosslinking agent.

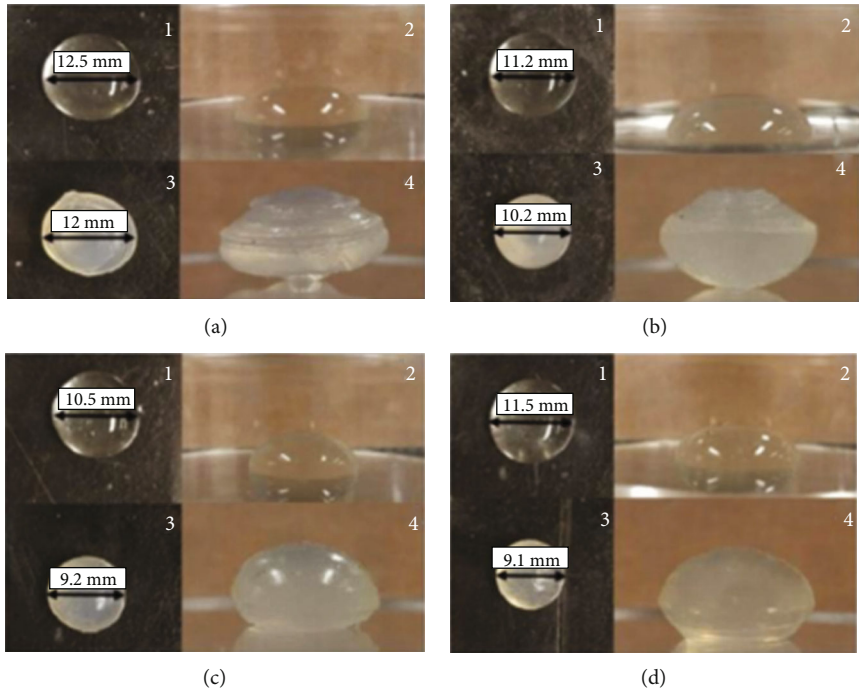

Figure 5: Effect of crosslinker concentration on gel retraction and appearance. Images of hydrogel discs crosslinked with (a) 0.1 M, (b) 0.5 M, (c) 1 M, and (d) 2 M $CaCl_2$ solution. Top images in each set represent gel precursor before the final crosslinking, and bottom images represent the resulting gel after crosslinking. The chitosan/CE conjugate ratio of the samples shown is 90 : 10, and the crosslinking time is 45 min for all samples.

component for strength enhancement in this formulation, and the average storage modulus increased from around 69.5 kPa to 112.3 kPa with increased CE. This could be ascribed to more carboxyl groups present in CE after modification, which clearly induced higher crosslinking density with calcium than pristine chitosan. In addition, the effect of crosslinking time on storage and loss modulus is illustrated in Figure 4(c). As expected, longer crosslinking time resulted in tighter polymer networks and higher storage and loss modulus.

Furthermore, crosslinking effect was investigated by measuring the shrinkage of the gels caused by crosslinking. To this end, four concentrations of calcium ranging from 0.1 to 2 M were considered. As the concentration of the crosslinking agent increased, a reduction in the diameter of the hydrogel disc (from 12 mm to 9.1 mm) was observed (Figure 5). In addition, gelation patterns on the hydrogel appear to be smoother with higher concentrations of calcium due to fast gelation.

To further study the effect of the crosslinker concentration, the compressive strength of hydrogels crosslinked with four concentrations of calcium solution was determined. The stress-strain curves and Young's modulus of the four groups were determined and presented in Figures 6(a) and 6(b). Higher crosslinking concentrations led to higher stiffness and lower elasticity which could be attributed to more restricted polymer networks and the shifting of the peak stresses to the right to yield higher strain. In addition, a six-fold increase in the peak stress was observed as calcium concentration was increased from 0.1 to 2 M. It can also be concluded from Figure 6(a) that the stiffness of the present bioink is tunable to provide the proper support. Furthermore, the effect of crosslinking concentration was studied by testing all the four samples for storage and loss modulus (Figure 6(c)). This figure also shows the tunability of viscoelastic properties of the hydrogel achieved by adjusting the crosslinking concentration. As expected, higher crosslinking concentration led to stronger polymer networks which in turn increased the storage and loss modulus.

Shear thinning, the reduction of viscosity by increased shear rate, is observed in Figure 6(d), and this verifies the non-Newtonian behavior of the hydrogel precursor. This phenomenon is often observed in solutions containing high molecular weight polymers. We observed that for higher concentrations, relative viscosity reduction was greater. The significant change in the shear thinning plots indicates the significance of the proportions of CE and chitosan as well as the implication of concentration changes.

3.3. Swelling Ratio. Due to high water content, hydrogels are considered biodegradable soft materials being able to mimic soft tissue. Due to their biodegradability and biocompatibility, hydrogels have found important applications in wound dressing [21], biomedical implants [22], cell studies, etc. To find out the suitability of any specific hydrogel for these types of applications, it is required to study the amount of water they can absorb over time. Swelling behavior of the hydrogel crosslinked by various crosslinker concentrations is studied and presented in Figure 6(e). Hydrogels were weighed before immersion in double-distilled water and weighed multiple

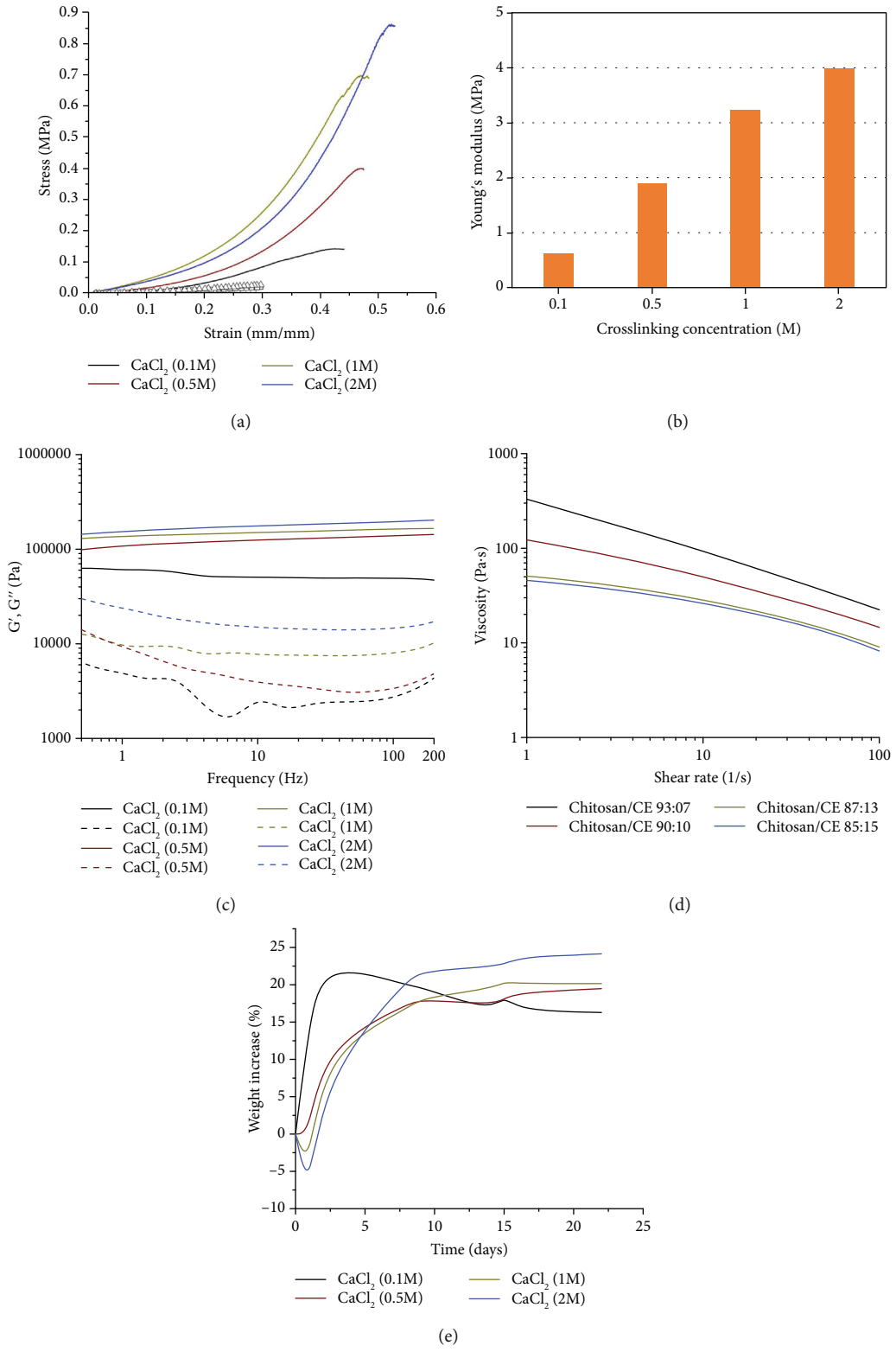

Figure 6: (a, b) Effect of crosslinker concentration on compressive strength of hydrogel and comparison with NFC/alginate hydrogel. (c) Storage modulus G' and loss modulus G'' of the bioink as a function of crosslinker concentration. Solid lines represent storage modulus, and dashed lines represent loss modulus. (d) Study of shear thinning properties of four chitosan/CE conjugate ratios. (e) Swelling ratio in samples crosslinked with four concentrations of calcium solution ranging from 0.1 M to 2 M. In (a–c) and (e), the chitosan/CE conjugate ratio of the samples tested was 90 : 10 and the crosslinking time was 45 min for all samples.

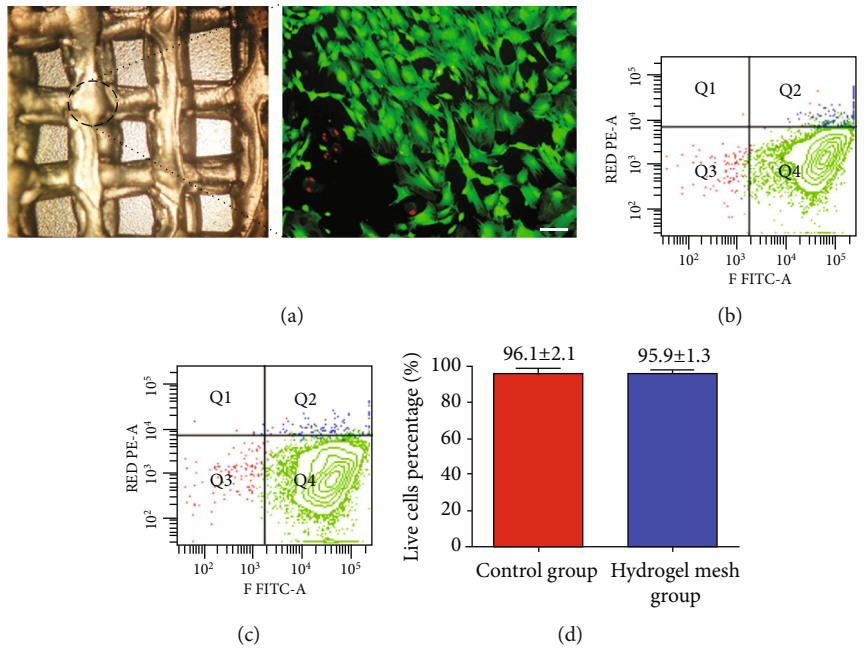

FIGURE 7: (a) Live/dead staining of chondrocytes. (b) Flow cytometry result of cell viability in the control group. (c) Flow cytometry result of cell viability in the hydrogel mesh group. (d) Quantification of cell viability in both groups. Scale bar = 100 μm.

times over a period of 22 days. As evident in the figure, hydrogels crosslinked with 1 M and 2 M calcium solution had a slightly decreased weight in the first day and start to absorb water from the second day. The small deswelling observed in higher concentrations could be attributed to pH or ionic strength change. The overall swelling trend reached a stable state which fell in the range of 14 to 24 percent of weight increase.

3.4. Evaluation of Chondrocyte Viability. The potential effects of the hydrogel mesh on cell viability were investigated (Figure 7). The samples used for all cell studies were prepared with a chitosan : CE ratio of 90 : 10 and crosslinked with 0.5 M calcium chloride solution. Chondrocyte viability was evaluated with the LIVE/DEAD Viability/Cytotoxicity Kit after 36 h of seeding on the hydrogel mesh. Live cells emitted green fluorescence in the cytoplasm, whereas nuclei of dead cells emitted red fluorescence. Only a small amount of apoptotic cells could be seen under fluorescence microscopy, indicating low cytotoxicity of the hydrogel. The cell viability was further evaluated by flow cytometry. The result demonstrated a similar live cell percentage in the hydrogel mesh group (95.9 ± 1.3%) and the control group (96.1 ± 2.1%), indicating that the hydrogel mesh did not affect the cell viability.

3.5. Evaluation of Chondrocyte Proliferation. After seeding on the scaffold for 36 h, chondrocyte proliferation status was assessed by EdU staining (Figure 8(a)). EdU-positive chondrocytes were detected in both groups, which indicate the proliferation of chondrocytes. Quantification of the chondrocyte proliferation status revealed a similar proliferation rate between the hydrogel mesh group (9.9 ± 0.7%) and the control (8.2 ± 1.4%) (Figure 8(b)), indicating that the hydrogel scaffold did not impair the proliferation of chondrocytes.

3.6. Expression of Chondrogenic Markers. The expression of chondrogenic markers was evaluated at different time points, including the ECM marker, collagen II (Figure 9(a)), and the chondrogenic transcription factor, Sox 9 (Figure 9(b)). As extracellular matrix protein of cartilage, collagen II expression reached its peak at day 6 in the mesh group and was higher than that in the control group between day 6 and day 12. The expression of the chondrogenic gene, Sox 9, reached its peak at day 6, and the relative expression of Sox 9 was higher in the hydrogel mesh group than in the control during the same period.

4. Conclusion

This study presents novel chitosan-based bioink mainly composed of chitosan-EDTA with physical crosslinking by calcium solution. Multilayer 3D mesh structures were 3D printed showing stability and high printing fidelity. Based on the presented results, the newly developed bioink exhibits suitable stability and mechanical properties as well as fast gelation and high printing precision. According to the rheology and mechanical testing results, the bioink viscoelastic properties and mechanical strength are tunable by adjustment of the proportions of the components which provides a platform to expand the application of the bioink in tissue engineering. Furthermore, cell studies with chondrocytes show that the bioink is biocompatible, and it supports cell proliferation as well as helps cells to retain their chondrogenic phenotype. Our results illustrate that the developed

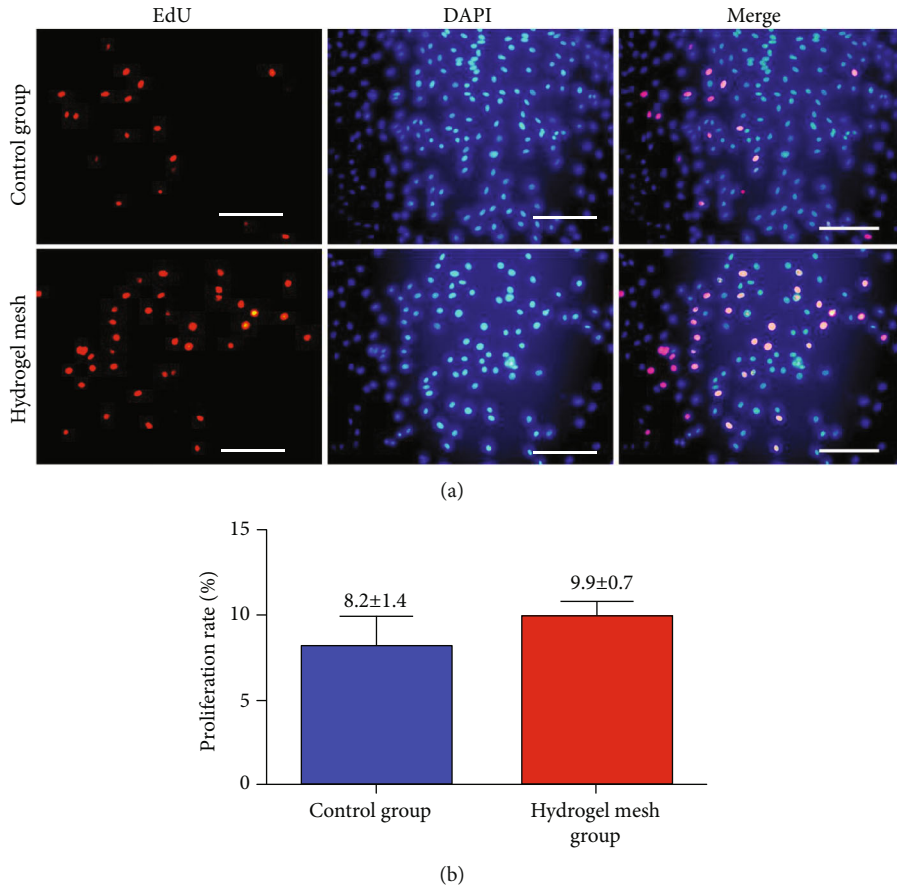

Figure 8: (a) EdU staining of chondrocytes in both groups. (b) Quantification of chondrocyte proliferation rate in both groups. Scale bar = 100 μm.

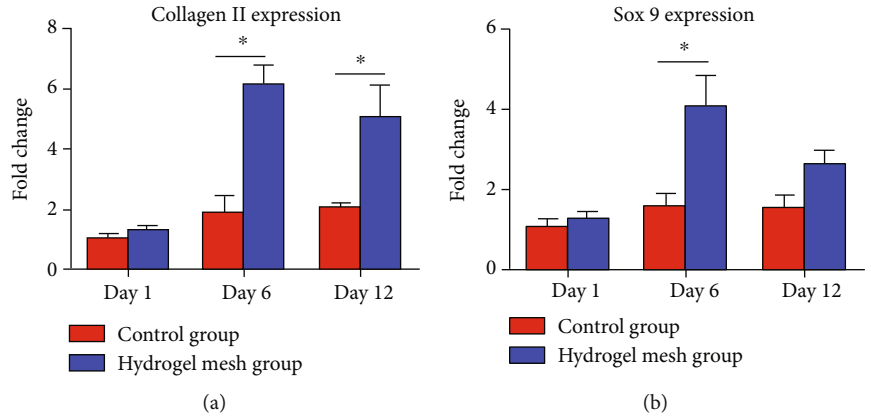

Figure 9: Chondrogenic marker expression. (a) Relative expression of collagen II. (b) Relative expression of Sox 9. $^*p < 0.05$.

bioink has the potential to be adopted for 3D bioprinting of scaffolds for tissue engineering.

Data Availability

The data used to support the findings of this study are included within the manuscript.

Conflicts of Interest

The authors report no conflicts of interest in this work.

Authors' Contributions

Yunfan He and Soroosh Derakhshanfar contributed equally and are co-first authors.

Acknowledgments

This work was supported by the National Nature Science Foundation of China (Grant No. 81660323). The present work was supported by the Natural Sciences and Engineering Research Council of Canada (NSERC) Discovery Grant, NSERC Accelerator Supplement Award, and Canada Foundation for Innovation.

References

[1] J. Malda, J. Visser, F. P. Melchels et al., "25th anniversary article: engineering hydrogels for biofabrication," *Advanced Materials*, vol. 25, no. 36, pp. 5011–5028, 2013.

[2] A. L. Rutz, K. E. Hyland, A. E. Jakus, W. R. Burghardt, and R. N. Shah, "A multimaterial bioink method for 3D printing tunable, cell-compatible hydrogels," *Advanced Materials*, vol. 27, no. 9, pp. 1607–1614, 2015.

[3] W. L. Ng, C. K. Chua, and Y.-F. Shen, "Print me an organ! Why we are not there yet," *Progress in Polymer Science*, vol. 97, p. 101145, 2019.

[4] J. M. Lee, W. L. Ng, and W. Y. Yeong, "Resolution and shape in bioprinting: strategizing towards complex tissue and organ printing," *Applied Physics Reviews*, vol. 6, no. 1, p. 011307, 2019.

[5] B. R. Ringeisen, R. K. Pirlo, P. K. Wu et al., "Cell and organ printing turns 15: diverse research to commercial transitions," *MRS bulletin*, vol. 38, no. 10, pp. 834–843, 2013.

[6] D. E. Discher, P. Janmey, and Y.-l. Wang, "Tissue cells feel and respond to the stiffness of their substrate," *Science*, vol. 310, no. 5751, pp. 1139–1143, 2005.

[7] M. P. Lutolf, F. E. Weber, H. G. Schmoekel et al., "Repair of bone defects using synthetic mimetics of collagenous extracellular matrices," *Nature Biotechnology*, vol. 21, no. 5, pp. 513–518, 2003.

[8] L. S. Nair and C. T. Laurencin, "Biodegradable polymers as biomaterials," *Progress in Polymer Science*, vol. 32, no. 8-9, pp. 762–798, 2007.

[9] J. W. Nichol, S. T. Koshy, H. Bae, C. M. Hwang, S. Yamanlar, and A. Khademhosseini, "Cell-laden microengineered gelatin methacrylate hydrogels," *Biomaterials*, vol. 31, no. 21, pp. 5536–5544, 2010.

[10] E. A. Phelps, N. O. Enemchukwu, V. F. Fiore et al., "Maleimide cross-linked bioactive peg hydrogel exhibits improved reaction kinetics and cross-linking for cell encapsulation and in situ delivery," *Advanced Materials*, vol. 24, no. 1, pp. 64–70, 2012.

[11] J. Maitra and V. K. Shukla, "Cross-linking in hydrogels-a review," *American Journal of Polymer Science*, vol. 4, no. 2, pp. 25–31, 2014.

[12] H. C. Liang, W. H. Chang, H. F. Liang, M. H. Lee, and H. W. Sung, "Crosslinking structures of gelatin hydrogels crosslinked with genipin or a water-soluble carbodiimide," *Journal of Applied Polymer Science*, vol. 91, no. 6, pp. 4017–4026, 2004.

[13] R. A. de Carvalho and C. R. F. Grosso, "Properties of chemically modified gelatin films," *Brazilian Journal of Chemical Engineering*, vol. 23, no. 1, pp. 45–53, 2006.

[14] K. Markstedt, A. Mantas, I. Tournier, H. M. Ávila, D. Hägg, and P. Gatenholm, "3D bioprinting human chondrocytes with nanocellulose–alginate bioink for cartilage tissue engineering applications," *Biomacromolecules*, vol. 16, no. 5, pp. 1489–1496, 2015.

[15] B. Sarker, R. Singh, R. Silva et al., "Evaluation of fibroblasts adhesion and proliferation on alginate-gelatin crosslinked hydrogel," *PLOS ONE*, vol. 9, no. 9, 2014.

[16] C. R. Chu, M. B. Millis, and S. A. Olson, "Osteoarthritis: from palliation to prevention: AOA critical issues," *The Journal of Bone and Joint Surgery. American volume*, vol. 96, no. 15, p. e130, 2014.

[17] J. Farr, B. Cole, A. Dhawan, J. Kercher, and S. Sherman, "Clinical cartilage restoration: evolution and overview," *Clinical Orthopaedics and Related Research®*, vol. 469, no. 10, pp. 2696–2705, 2011.

[18] J.-Y. Lee, S.-H. Nam, S.-Y. Im et al., "Enhanced bone formation by controlled growth factor delivery from chitosan- based biomaterials," *Journal of Controlled Release*, vol. 78, no. 1-3, pp. 187–197, 2002.

[19] D. L. Nettles, S. H. Elder, and J. A. Gilbert, "Potential use of chitosan as a cell scaffold material for cartilage tissue engineering," *Tissue Engineering*, vol. 8, no. 6, pp. 1009–1016, 2002.

[20] G. D. Nicodemus and S. J. Bryant, "Cell encapsulation in biodegradable hydrogels for tissue engineering applications," *Tissue Engineering Part B: Reviews*, vol. 14, no. 2, pp. 149–165, 2008.

[21] M. Rahimnejad, S. Derakhshanfar, and W. Zhong, "Biomaterials and tissue engineering for scar management in wound care," *Burns & Trauma*, vol. 5, no. 1, p. 4, 2017.

[22] D. Seliktar, "Designing cell-compatible hydrogels for biomedical applications," *Science*, vol. 336, no. 6085, pp. 1124–1128, 2012.